Study of the radiation damage of Silicon Photo-Multipliers at the GELINA facility

2014 JINST 9 P04004

(http://iopscience.iop.org/1748-0221/9/04/P04004)

Jinst

PUBLISHED BY IOP PUBLISHING FOR SISSA MEDIALAB

RECEIVED: *December 23, 2013*
ACCEPTED: *February 24, 2014*
PUBLISHED: *April 4, 2014*

Study of the radiation damage of Silicon Photo-Multipliers at the GELINA facility

M. Andreotti,[a,b] **W. Baldini,**[b] **R. Calabrese,**[a,b] **G. Cibinetto,**[b] **A. Cotta Ramusino,**[b] **C. De Donato,**[g,h] **R. Faccini,**[i,j] **M. Fiorini,**[a,b] **E. Luppi,**[a,b] **R. Malaguti,**[b] **A. Montanari,**[d] **A. Pietropaolo,**[f] **V. Santoro,**[a,b] **G. Tellarini,**[a,b,1] **L. Tomassetti**[b,c] **and N. Tosi**[d,e]

[a]*Dipartimento di Fisica e Scienze della Terra, Università di Ferrara, Ferrara, Italy*
[b]*INFN-Ferrara, Ferrara, Italy*
[c]*Dipartimento di Matematica e Informatica, Università di Ferrara, Ferrara, Italy*
[d]*INFN-Bologna, Bologna, Italy*
[e]*Dipartimento di Fisica, Università di Bologna, Bologna, Italy*
[f]*Enea, Roma, Italy*
[g]*Dipartimento di Fisica, Università di Roma Tor Vergata, Roma, Italy*
[h]*INFN-Roma Tor Vergata, Roma, Italy*
[i]*Dipartimento di Fisica, Roma Università La Sapienza , Roma, Italy*
[j]*INFN-Roma, Roma, Italy*

E-mail: tellarini@fe.infn.it

ABSTRACT: In this paper we present a study of the neutrons-induced damage in Silicon Photo-Multipliers. Twenty-six devices, produced by AdvanSiD, Hamamatsu and SensL, have been irradiated at the Geel Electron LINear Accelerator (GELINA) in Belgium with a nearly white neutron beam. The total 1 MeV equivalent integrated dose was $6.2 \times 10^9\ \mathrm{n_{eq}/cm^2}$. Photodetector performances have been measured during the whole irradiation period and a gradual worsening of the detector properties, such as dark current and charge spectra, has been observed.

An extensive comparison of the performances of all the tested devices will be presented.

KEYWORDS: Radiation damage to detector materials (solid state); Photon detectors for UV, visible and IR photons (solid-state) (PIN diodes, APDs, Si-PMTs, G-APDs, CCDs, EBCCDs, EMCCDs etc)

[1]Corresponding author.

doi:10.1088/1748-0221/9/04/P04004

2014 JINST 9 P04004

Contents

1 Introduction

A Silicon Photo-Multiplier (henceforth called SiPM) is a novel semiconductor photo-detector composed by a matrix of hundreds of pixels operating a few volts above the breakdown voltage (Geiger-Mode Avalanche Photo-Diode). Distinctive features of such technology are: single photon detection capability, high gain $\left(\approx 10^6\right)$ and good time resolution $\left(< 1\,\mathrm{ns}\right)$ [1]. In addition SiPMs are small sized, insensitive to magnetic fields and relatively cheap. For these reasons SiPMs are increasingly used in all those fields that require an efficient photons detection (i.e. Astrophysics, Nuclear Medicine, High Energy Physics, . . .).

SiPMs still have a few drawbacks though: a rather high dark noise and a strong sensitivity to radiation, especially neutrons. The former issue is being addressed and in the latest years the manufacturers reduced it considerably. The latter is still an open issue for the use of SiPMs, especially in high energy physics experiments, where a very high radiation exposure is expected.

Different studies have shown a correlation between the bulk defects in the silicon structure due to the radiation damage and the deterioration of the photo-detector performances [2, 3]. Hadrons and high energy leptons are able to produce point defects as well as cluster-related defects in the active volume of the photo-detector. In particular neutrons traveling within the silicon lattice induce many displacements of silicon atoms that at the end of the path form a disordered agglomeration of atoms called cluster [4–6]. From the macroscopic point of view, some of these defects act as charge carriers generator centers, producing an increase of dark noise.

In high energy physics experiments neutrons are produced by photo-nuclear reactions of X and γ rays with the surrounding media [7]. The energy spectrum of the emitted neutrons is broadened from thermal energies up to a few MeV. Therefore, measuring the performance degradation on a neutron beam that can reproduce the energy spectrum of the neutron cloud is of primary interest for the development of future particle physics detectors.

2014 JINST 9 P04004

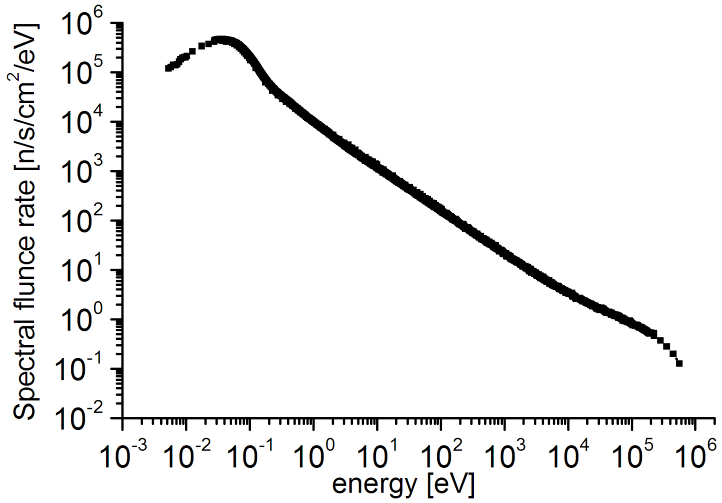

Figure 1. Neutrons spectrum at the GELINA facility at 10m from the water-Berillium moderator.

2 The GELINA facility

The irradiation test has been performed at the Geel Electron LINear Accelerator (GELINA), at the Institute for Reference Materials and Measurements (IRMM) in Geel (BE). A 100 MeV pulsed electron beam impinges on a rotating target composed by Uranium (90 %) and Molibdenum (10 %) [8]; the decelerated electrons produce high energy photons via bremsstrhalung, which, in turn, have photonuclear reactions (γ,n) with the Uranium nuclei inducing neutron emission. The produced neutrons are then moderated in a Berillium-Water tank generating the energy spectrum shown in figure 1.

The outgoing moderated beam extents from 20 meV to 2 MeV featuring a Maxwellian peak at 40 meV and a $\approx 1/E$ energy tail. The GELINA facility has 12 test lines (called "flight path") with experimental rooms at different distances from the neutrons source [9]. Our irradiation test has been carried out at a distance of 10 m from the Uranium target, where the beam diameter was about 5 cm. During the test the average electron current was 35 μA, producing a neutron flux of about 7×10^5 n/cm^2/s.

The total integrated dose has been calculated using offline calibrations performed by the facility personnel by means of the signal coming from a boron counter, placed in the proximity of the neutron source. Few cm of lead were added to reduce the contamination of the photons produced in the target; the lead attenuation has been checked with both, measurements and simulations and was included in the total dose calculation. The total integrated dose has been estimated to be about 3.2×10^{10} n/cm^2 in the entire energy range, corresponding to about 6.2×10^9 n_{eq}/cm^2 1 MeV equivalent neutrons.[1]

3 The experimental setup

Twenty-six SiPMs have been tested. They are squared devices with different area and pixel size produced by: AdvanSiD [10], HAMAMATSU [11] (called Multi Pixel Photon Counter or MPPC)

[1] The 1 MeV equivalent dose has been calculated normalizing the measured neutron energy spectra with the Non Ionizing Energy Loss (NIEL) curve for Silicon.

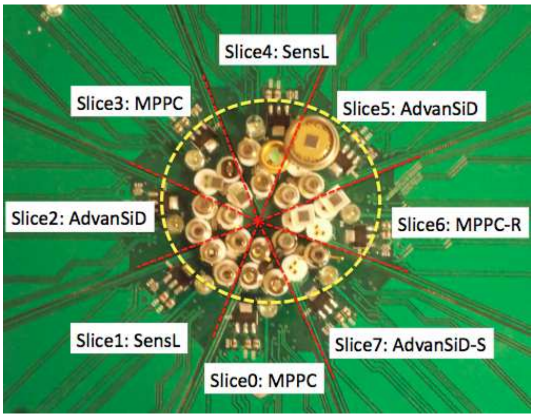

Figure 2. Picture of the irradiated SiPMs mounted on the supporting PCB.

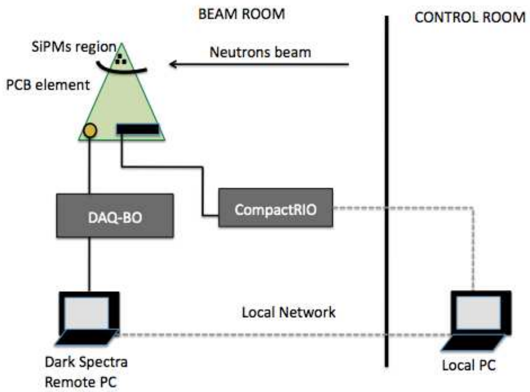

Figure 3. Schematic representation of the readout system.

and SensL [12]. The SiPMs were housed on eight triangular custom made Printed Circuit Boards (as shown in figure 2), joined together on a supporting aluminum structure. The photodetectors were located at the center of the structure within a radius of about 2.5 cm, which corresponds to the effective dimension of the beam. In table 1 is reported the complete list of the tested SiPMs.

During the test, the SiPMs were biased with a common voltage for each PCB element that contains SIPMs of the same brand, provided by a EHQ 8210x-F power supply produced by ISEG [13], plus a fine individual correction, provided by a 12-bits Digital to Analog Converter. For each SiPM the nominal voltage reported by the manufacturer has been selected. The measurement of the current was performed by sensing the voltage drop on a 2 kΩ resistor and was carried out by a 16-bit analog input readout module, controlled by a National Instruments CompactRIO acquisition system [14]. The accuracy on the current measurement was about 0.01 μA.

We also measured the SiPMs dark charge spectra, thanks to a custom made data acquisition system developed by the INFN Bologna laboratory [15]. This system received a copy of the analog signal from a subset of 8 SiPMs; the signal was amplified and shaped (with a 70 ns shaping time) then digitized by an ADC. Photodetectors temperature has been measured online by means of four temperature probes placed near the SiPMs site. The beam parameters were also recorded for offline analysis. In figure 3 a schematic view of the readout system is reported.

4 Dark currents and I-V characteristic curves

For each device we measured the dark current as a function of the integrated dose during the whole irradiation process. The increase of SiPMs dark current is expected to be linear with respect to the radiation fluence, as described by eq. (4.1):

$$\Delta i_{\mathrm{Dark}} \approx (\alpha \cdot V_{\mathrm{eff}} \cdot G \cdot K_{\mathrm{NIEL}}) \cdot \Phi = (\alpha \cdot V_{\mathrm{eff}} \cdot G) \cdot \Phi_{\mathrm{eq}} \tag{4.1}$$

where α is the dark current damage constant for Silicon, G the SiPM gain and $\Phi_{\mathrm{eq}} = K_{\mathrm{NIEL}}\ \Phi$ the 1 MeV equivalent neutron fluence. $V_{\mathrm{eff}} = A_{\mathrm{SiPM}} \cdot d_{\mathrm{eff}} \cdot FF$ is the effective volume being FF the geometric fill factor and d_{eff} the effective thickness of the active volume [16, 17]. We have then

Table 1. Table of irradiated SiPMs. The suffix A stands for AdvanSiD, H for Hamamatsu and S for SensL; the first number defines the active area (1, 1.3 or 3.0 mm), the second (25, 50 or 100 μm) defines the pixel dimension while the last is our serial number. Within the irradiated SiPMs set there are four non-commercial prototypes labelled with the final letter R for Hamamatsu and S for Advansid. For each SiPM are also reported the bias voltage, the area, the pixel size, the integrated dose and the 1 MeV neutron equivalent dose.

Brand	**Code**	$\mathbf{V_{bias}}$ (Volt)	**Area** (mm^2)	**Pixel Size** (μm)	**Int. dose** 10^{10} n/cm^2	**Eq. dose** 10^9 n_{eq/cm^2}
HAMAMATSU	$H1-50\_02$	-71.0	1	50	2.8	5.4
HAMAMATSU	$H1-100\_41$	-70.6	1	100	2.8	5.4
HAMAMATSU	$H1-25\_05$	-74.0	1	25	2.8	5.4
SensL	$S1-50\_26$	-29.1	1	50	3.2	6.2
SensL	$S1-100\_30$	-29.1	1	100	3.2	6.2
SensL	$S1-20\_29$	-29.1	1	20	3.2	6.2
AdvanSiD	$A1-50\_11$	-31.0	1	50	3.2	6.2
AdvanSiD	$A1-100\_19$	-32.0	1	100	3.2	6.2
AdvanSiD	$A1-25\_20$	-32.0	1	25	3.2	6.2
HAMAMATSU	$H3-50\_10$	-72.5	9	50	3.2	6.2
HAMAMATSU	$H3-50\_08$	-72.5	9	50	2.8	6.2
HAMAMATSU	$H1.3-50\_07$	-71.2	1.69	50	3.2	6.2
SensL	$S1-35\_34$	-29.5	1	35	3.2	6.2
SensL	$S1-50\_27$	-29.5	1	50	3.2	6.2
SensL	$S3-35\_32$	-29.1	9	35	3.2	6.2
AdvanSiD	$A1-25\_37$	-33.9	1	25	3.2	6.2
AdvanSiD	$A3-50\_21$	-30.1	9	50	3.2	6.2
AdvanSiD	$A1-50\_13$	-32.0	1	50	3.2	6.2
HAMAMATSU	$H3-50\_17R$	-62.0	9	50	3.2	6.2
HAMAMATSU	$H3-100\_16R$	-61.1	9	100	3.2	6.2
AdvanSiD	$A1-50\_39S$	39.9	1	50	3.2	6.2
AdvanSiD	$A1-50\_40S$	39.9	1	50	3.2	6.2
HAMAMATSU	$H1-50\_04$	-71.0	1	50	0.39	0.76
HAMAMATSU	$H1-100\_00$	-70.6	1	100	0.39	0.76
HAMAMATSU	$H1-25\_06$	-74.0	1	25	0.39	0.76
HAMAMATSU	$H3-50\_09$	-72.5	9	50	0.39	0.76

performed a linear fit of the dark current versus the integrated dose to quantitatively compare the rate of change of the different devices.

We measured also the characteristic curve, dark current versus bias voltage (I-V curve), at different integrated dose. Figure 4 shows, for three 1×1 mm^2 devices, the I-V curves at the beginning of the irradiation test, at the end, and after four months of recovery at room temperature. A self-annealing of the SiPMs is clearly visible.

The dark current of a Silicon Photomultiplier depends on the temperature [19], we have then recorded the temperature of the devices during the whole test period, to perform a correction during

2014 JINST 9 P04004

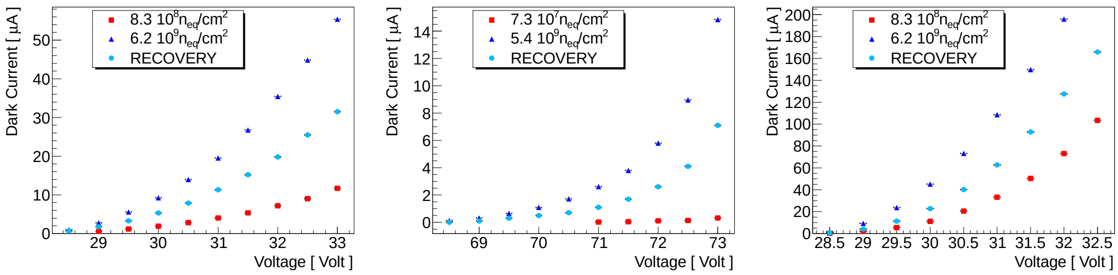

(a) AdvanSiD. **(b)** HAMAMATSU. **(c)** SensL.

Figure 4. Characteristic curves for three SiPMs $1 \times 1\,\mathrm{mm}^2$ produced by AdvanSiD, HAMAMATSU and SensL.

the offline data analysis. The average temperature has been of 25.5°C. In order to study the effect of temperature on the SiPMs dark current we have measured the temperature for a night without irradiation. The effect is specific for each SiPM (manufacturers, area ecc.) but on the average it is around a 10% of variation in the dark current for a ΔT of 2°C. Given the small variation (2°C maximum between day and night), the effect has been found to be negligible for the trend of the dark current with respect to the integrated dose.[2]

5 Comparative analysis

The possibility to perform simultaneous measurements on different SiPMs, in the same experimental conditions, allows a direct and very interesting comparison among devices with different geometries and of different producers. Here is the list of comparisons that will be presented in this section:

- Area $1 \times 1\,\mathrm{mm}^2$ and different pixel size;
- Area $1 \times 1\,\mathrm{mm}^2$ and different brand;
- Area $3 \times 3\,\mathrm{mm}^2$, pixel size $50\,\mu$m and different brand;
- Standard MPPC vs Radiation Hard MPPC.

Area $1 \times 1\,\mathrm{mm}^2$ and different pixel size. Figure 5 shows the direct comparison of the dark currents for nine $1 \times 1\,\mathrm{mm}^2$ devices. As expected [22], starting from $\approx 10^8\,\mathrm{n_{eq}}/\mathrm{cm}^2$ is clearly visible a change in the speed at which the dark current increases with the accumulated dose for all the tested SiPMs. In general, we noticed the Hamamatsu devices to be sligtly more sensitive to radiation, as the deterioration starts at about $0.2 \times 10^8\,\mathrm{n_{eq}}/\mathrm{cm}^2$, and with a higher slope. AdvansiD and SensL, on this side, were slightly more robust, as the change started at approximately $2 \times 10^8\,\mathrm{n_{eq}}/\mathrm{cm}^2$. We should also notice though, that the Hamamatsu initial performances, like dark current (and dark noise), were about 10 times lower, so the final balance is not well defined.

[2]It has been checked on a few devices.

2014 JINST 9 P04004

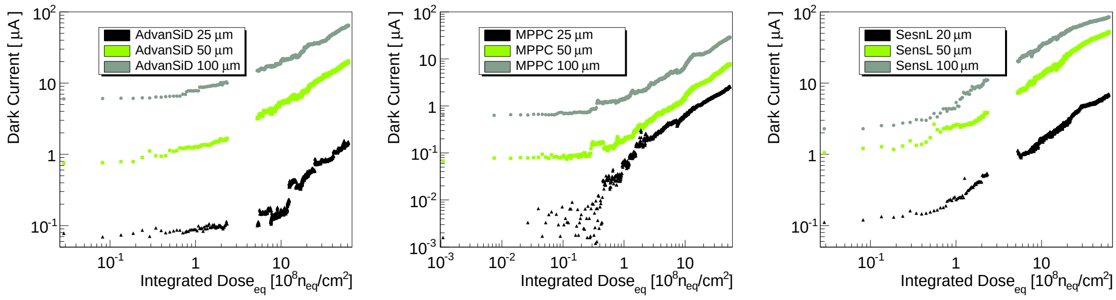

(a) AdvanSiD. **(b)** HAMAMATSU. **(c)** SensL.

Figure 5. Dark currents versus the integrated dose for SiPMs with area of $1 \times 1\,\text{mm}^2$ and different pixel size. The missing points on AdvansiD and SensL are due to some problems with the DAQ.

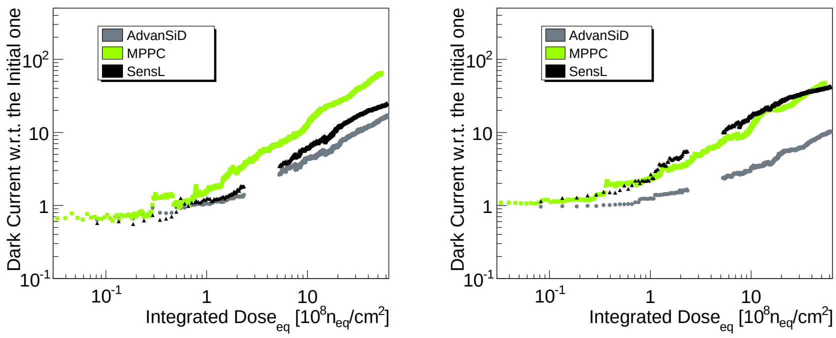

(a) Pixel size: $50\,\mu$m. **(b)** Pixel size: $100\,\mu$m.

Figure 6. Dark currents versus the integrated dose for SiPMs with area of $1 \times 1\,\text{mm}^2$ and different brands.

As far as different geometries (especially pixel size) is concerned, apart from the expected different values in dark currents, we could not measure any significant difference in the trends of the radiation damage vs dose.

Area $1 \times 1\,\text{mm}^2$ and different brand. Figure 6 shows the normalized dark current versus the accumulated dose for six SiPMs with the same geometrical dimensions $(1 \times 1\,\text{mm}^2$, $50\,\mu$m (6a) and $100\,\mu$m (6b)) produced by AdvanSiD, HAMAMATSU and SensL. From figure 6a we can see that the dark current change is slightly lower for the device produced by AdvansiD and higher for the other two producers. This behavior is confirmed also considering SiPMs with pixel size of $100\,\mu$m (see figure 6b). In table 2 the ratio between the final value of the dark current and the initial one (i_f/i_0) provides a quantitative idea of what is described above. In addition, from the linear fit to the normalized dark current with respect to the integrated dose, the angular coefficient can be calculated (also reported in table 2), that well reproduces the scenario represented in the plots.

Area $3 \times 3\,\text{mm}^2$, pixel size $50\,\mu$m and different brand. In figure 7 the normalized dark current is reported, as a function of the fluence, for $3 \times 3\,\text{mm}^2$ and pixel size of $50\,\mu$m, for AdvansiD and Hamamatsu devices. MPPCs are more sensitive to the radiation damage, as we can see also in table 3 where the ratio i_f/i_0 is reported for the three SiPMs. From the linear fit it can be seen that also the angular coefficient is higher for the MPPCs.

2014 JINST 9 P04004

Table 2. Ratio i_f/i_0 and angular coefficient of the linear fit for SiPMs with pixel size of 50 μm, 100 μm and area 1×1 mm^2.

SiPM	$\mathbf{i_f/i_0}$	**ang.coeff** $[10^{-8}\,\mu\text{Acm}^2]$
$A1-50\_11$	17	0.25
$H1-50\_02$	67	1.09
$S1-50\_26$	25	0.39
$A1-100\_19$	10	0.14
$H1-100\_41$	47	0.75
$S1-100\_30$	42	0.54

Table 3. Ratio i_f/i_0 for SiPMs with pixel size of 50 μm and area 3×3 mm^2.

SiPM	$\mathbf{i_f/i_0}$	**ang.coeff** $[10^{-8}\,\mu\text{Acm}^2]$
$A3-50\_21$	12	0.18
$H3-50\_08$	84	1.32
$H3-50\_10$	92	1.36

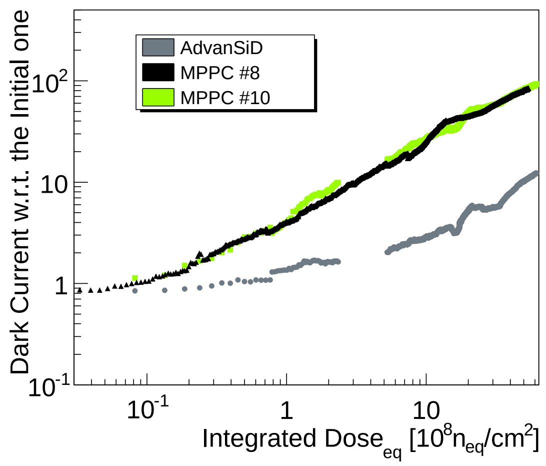

Figure 7. Dark currents versus the integrated dose for three SiPMs with an area of 3×3 mm^2 and a pixel size of 50 μm.

Radiation Hard MPPCs vs Standard MPPCs

Within our sample we had also two non-commercial MPPCs (that we will call Radiation Hard) provided by Hamamatsu. They had an area of 3×3 mm^2 and pixel size of 50 μm and 100 μm. It's interesting to compare the variation of their performances with respect to stardand devices. Figure 8 shows the comparison between two Standard MPPCs ($H3-50\_08$ and $H3-50\_10$) and the corresponding Radiation Hard ($H3-50\_17R$) device.

From the point of view of dark current, all three devices have similar trends. More interesting is the behaviour of SiPMs (coupled with Wavelength Shifting fibers) as scintillator read-out with

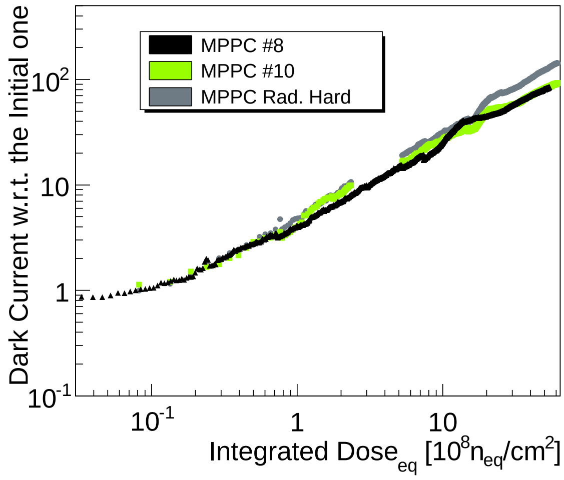

Figure 8. Dark currents versus the integrated dose for two standard MPPCs and one Radiation Hard MPPC.

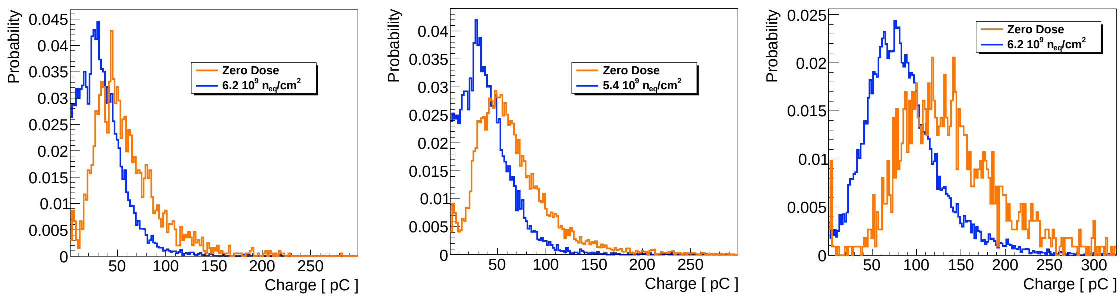

(a) Standard MPPC: $H3-50\_10$.

(b) Standard MPPC: $H3-50\_08$.

(c) Radiation Hard MPPC: $H3-50\_17R$.

Figure 9. Cosmic rays charge spectra before and after the irradiation for three devices with an area of $3\times3\,\mathrm{mm}^2$ and a pixel size of $50\,\mu$m.

cosmics. Figure 9 shows the charge spectra from cosmic rays, before (orange) and after (blue) the irradiation, recorded in the Ferrara Laboratory with a simple setup (a coincidence of scintillators). It can be seen that the Radiation Hard device (figure 9c) shows an initial higher gain that, after the irradiation, still allow to distinguish the signal, while for the standard devices (figure 9a, 9b) this possibility is considerably reduced.

Given the above results, more studies are currently being performed on several Rad. Hard devices provided by Hamamatsu.

6 Dark charge spectra

During our test we also measured the dark noise spectra for a representative subset (8 devices) of the sample. We used a random trigger and collected 10^5 events for each measurement. The dark spectra before irradiation are shown in figure 10. All spectra show very clearly the pedestal peak, followed by the single pixel peak and some multiple-pixel peaks. At an irradiation level of

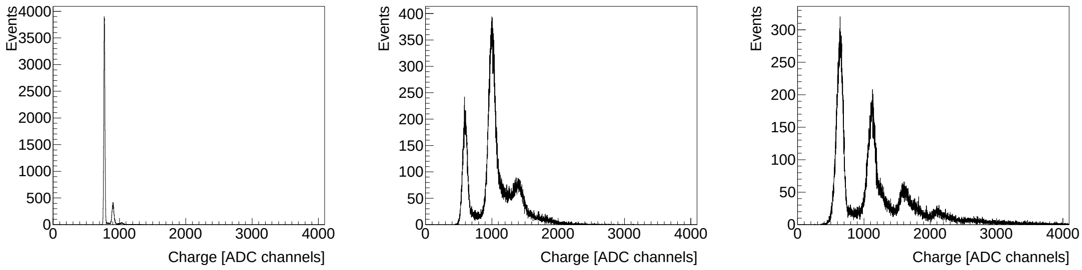

(a) Hamamatsu. **(b)** AdvanSiD. **(c)** SensL.

Figure 10. Dark Charge Spectra before irradiation for three SiPMs of area $1 \times 1\,\text{mm}^2$, pixel size $50\,\mu$m and different brands.

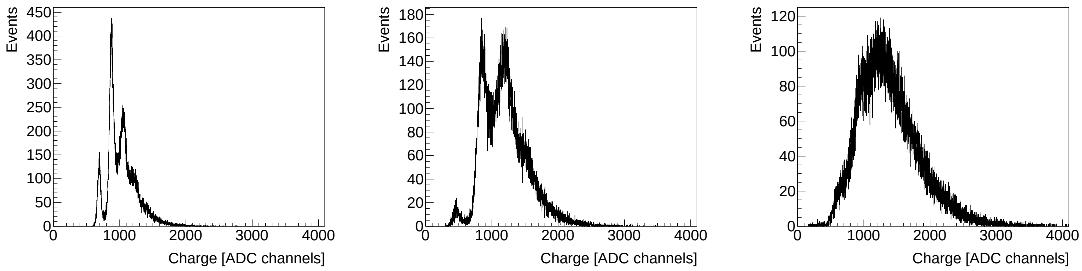

(a) Hamamatsu. **(b)** AdvanSiD. **(c)** SensL.

Figure 11. Dark Charge Spectra after irradiation with $3.3 \times 10^8\,\text{n}_{\text{eq}}/\text{cm}^2$ for three SiPMs of area $1 \times 1\,\text{mm}^2$, pixel size $50\,\mu$m and different brands.

$3.3 \times 10^8\,\text{n}_{\text{eq}}/\text{cm}^2$, the spectra have noticeably changed, as can be seen from figure 11. All devices show some amount of performance degradation: some still have clearly recognizable structure, while others have already lost the individual peaks. It is important to notice that, for the devices where it can still be accurately measured, no substantial variation is observed in the gain. A drift of the pedestal position, as described already in previous sections, is instead observed for all devices. Finally, after $2.2 \times 10^9\,\text{n}_{\text{eq}}/\text{cm}^2$, no structure is visible in the spectrum of any device, as can be seen in figure 12; it is therefore impossible to measure the position of the pedestal peak and calculate the gain.

This loss of photon counting capability is mainly due to the increase of the dark noise and to a significant worsening of the gain uniformity which, in turn, causes a wide broadening (and overlapping) of the different photoelectron peaks.

7 Conclusions

We have studied neutrons-induced radiation damage on a set of twenty-six Silicon Photo-Multipliers, from AdvansiD, Hamamatsu, SensL at the GELINA facility in Belgium. The effects of an accumulated dose of $3.2 \times 10^{10}\,\text{n}/\text{cm}^2$ (which corresponds to $6.2 \times 10^9\,\text{n}_{\text{eq}}/\text{cm}^2$ 1 MeV equivalent neutrons) have been measured online during the irradiation.

In general, as expected, starting from $\approx 10^8\,\text{n}_{\text{eq}}/\text{cm}^2$ is clearly visible a large increase of dark current and a significant loss in single photon counting capability.

2014 JINST 9 P04004

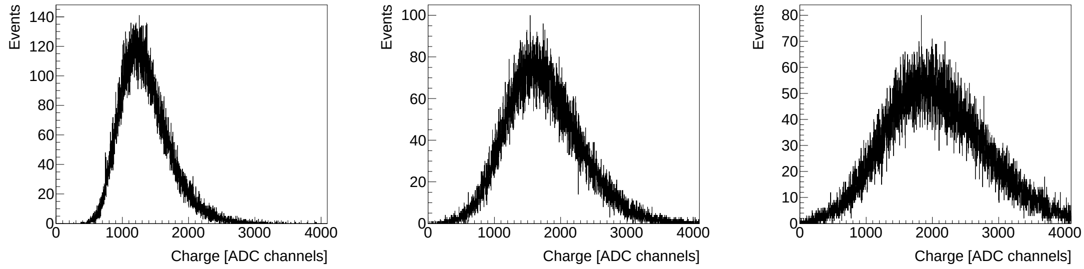

(a) Hamamatsu. **(b)** AdvanSiD. **(c)** SensL.

Figure 12. Dark Charge Spectra after irradiation with $2.2 \times 10^9\ \mathrm{n_{eq}/cm^2}$ for three SiPMs of area $1 \times 1\ \mathrm{mm}^2$, pixel size $50\,\mu$m and different brands.

We noticed the Hamamatsu devices to be sligtly more sensitive to radiation, as the deterioration starts at about $0.2 \times 10^8\ \mathrm{n_{eq}/cm^2}$, and with a higher slope. AdvandiD and SensL, on this side, were slightly more robust, as the change started at approximately $2 \times 10^8\ \mathrm{n_{eq}/cm^2}$. We should also notice though, that the Hamamatsu initial performances, like dark current (and dark noise), were about 10 times lower, so the final balance is not well defined.

As far as different geometries (especially pixel size) are concerned, apart from the expected different values in dark currents, we could not measure any significant difference in the trends of the radiation damage vs dose.

As for the so colled Radiation Hard devices (Hamamatsu) we noticed a better behaviour (w.r.t. standard ones) from the point of view of the signal from cosmics. This was essentially due to the higher pre-irradiation value of the gain, which allowed the cosmic signal to be still visible after the irradiation. More studies in this direction are being carried out in collaboration with Hamamatsu.

Finally, from the point of view of the photon counting capability, we didn't notice large differences among the manufacturers, with Hamamatsu performing perhaps slightly better.

Acknowledgments

The authors would like to gratefully thank the techical staff of the INFN, ENEA and of all the Universities involved in the project: Bologna, Ferrara, Rome La Sapienza, Rome Tor Vergata. A particular acknowledgment goes to the personnel of the IRMM-GELINA facility, for their fundamental support (and patience) which made the realization of the test possible.

References

[1] E. Guschin et al., *Multi-pixel Geiger-mode avalanche photodiodes with high quantum efficiency and low excess noise factor*, *Nucl. Instrum. Meth.* **A 567** (2006) 240.

[2] J.R. Srour, C.J. Marshall and P.W. Marshall, *Review of Displacement Damage Effects in Silicon Devices*, *IEEE Trans. Nucl. Sci.* **50** (2003) 653.

[3] M. Moll, *Radiation damage in silicon particle detectors: microscopic defects and macroscopic properties*, Ph.D. Thesis, University of Hamburg, Hamburg, Germany (1999), DESY-THESIS-1999-040.

2014 JINST 9 P04004

[4] M. Huhtinen, *Simulation of non-ionising energy loss and defect formation in silicon*, *Nucl. Instrum. Meth.* **A 491** (2002) 194.

[5] I. Pintiliea, G. Lindstroem, A. Junkes and E. Fretwurst, *Radiation Induced Point and Cluster-Related Defects with Strong Impact to Damage Properties of Silicon Detectors*, *Nucl. Instrum. Meth.* **A 611** (2009) 52 [arXiv:0907.3050].

[6] K. Gill, G. Hall and B. MacEvoy, *Bulk damage effects in irradiated silicon detectors due to clustered divacancies*, *J. Appl. Phys.* **82** (1997) 126.

[7] International Atomic Energy Agency, *Handbook of photonuclear data for applications. Cross-sections and spectra*, IAEA TECDOC 1178 (2000).

[8] W. Mondelaers and P. Schillebeeckx, *GELINA, a neutron time-of-flight facility for high-resolution neutron data measurements, Notiziario Neutroni e Luce di Sincrotrone* **11** (2006) 19.

[9] irmm.jrc.ec.europa.eu.

[10] http://www.advansid.com/.

[11] http://www.hamamatsu.com/us/en/4004.html.

[12] http://sensl.com/products/silicon-photomultipliers/.

[13] http://www.iseg-hv.com/en/products/.

[14] http://www.ni.com/compactrio.

[15] G. Balbi et al., *A versatile readout and control system for Silicon photomultipliers*, *IEEE Nucl. Sci. Symp. Med. Imag. Conf. Rec.* (2011) 918.

[16] Y. Musienko, D. Renker, Z. Charifoulline, K. Dieters, S. Reucroft and J. Swain, *Study of radiation damage induced by 82 MeV protons on multipixel Geiger-Mode avalanche photodiodes*, *Nucl. Instrum. Meth.* **A 610** (2009) 87.

[17] Y. Musienko, *State of the art in SiPM's*, *SiPM workshop*, CERN (2011).

[18] R. Greim et al., *Silicon photomultiplier arrays — a novel photon detector for a high resolution tracker produced at FBK-irst, Italy*, *Nucl. Phys. Proc. Suppl.* **197** (2009) 83 [arXiv:0903.3883].

[19] M. Ramilli, *Characterization of SiPM: temperature dependencies*, *IEEE Nucl. Sci. Symp. Conf. Rec.* (2008) 2467.

[20] G. Lindström, M. Moll and E. Fretwurst, *Radiation hardness of silicon detectors: A challenge from high-energy physics*, *Nucl. Instrum. Meth.* **A 426** (1999) 1.

[21] Y. Qiang, C. Zorn, F. Barbosa and E. Smith, *Radiation Hardness Tests of SiPMs for the JLab Hall D Barrel Calorimeter*, *Nucl. Instrum. Meth.* **A 698** (2013) 234 [arXiv:1207.3743].

[22] M. Angelone et al., *Silicon Photo-Multiplier radiation hardness tests with a beam controlled neutron source*, *Nucl. Instrum. Meth.* **A 623** (2010) 921 [arXiv:1002.3480].